Nanostructures

DOI: 10.1002/ange.200803202

Shape-Controlled Synthesis of Gold Nanoparticles in Deep Eutectic Solvents for Studies of Structure–Functionality Relationships in Electrocatalysis**

Hong-Gang Liao, Yan-Xia Jiang, Zhi-You Zhou, Sheng-Pei Chen, and Shi-Gang Sun**

Gold-based catalysts have attracted intense interest in recent years following the discovery[1] that small supported Au nanoparticles (NPs) can be effective catalysts for CO oxidation at low temperatures. Gold-based catalysts have been widely used and are regarded as a new generation of catalysts.[2] The properties of Au NPs depend strongly on their size and shape, which determine the surface structure of the particles. Fundamental studies of single-crystal planes of face-centered-cubic (fcc) metals demonstrated that the high-index planes possess a high density of low coordination number step atoms in comparison with low-index planes such as {111}, {100}, and even {110}, and therefore exhibit high activity for breaking chemical bonds.[3] Tian et al.[4] reported recently that tetrahexahedral-shaped Pt NPs display high catalytic activity and stability, as the tetrahexahedral Pt nanoparticle is bounded by a {730} surface and other high-index facets. Although the shape-controlled synthesis of Au NPs has been extensively studied,[5] the procedures often involve surfactants and Au seeds in solutions. Moreover, the shapes of the synthesized Au NPs are mainly cubes, tetrahedra, octahedra, and rhombic dodecahedra that are enclosed by low-index facets. Several starlike Au NPs bounded with low-index (111) facets have also been reported recently, but their shapes are not uniform and perfect.[6,7] It is known from crystal growth law that the growth rate along the direction perpendicular to the high-index planes is usually much faster than that to the low-index planes, so the high-index planes will be eliminated gradually during the crystal growth. Therefore, it is always challenging to develop shape-controlled syntheses of NPs bounded with high-index facets.

Deep eutectic solvents (DESs)[8] were first reported by Abbott and co-workers. They found that substituted quaternary ammonium salts mixed with hydrogen-bond donors such as amides can form liquids at ambient temperatures. These liquids have properties similar to those of ionic liquids, namely, high conductivity, viscosity, surface tensions, polarity, and thermal stability and negligible vapor pressure. Unlike the ionic liquids, DESs can nevertheless be easily prepared at low cost and with high purity. Some of the hydrogen-bond donors are common bulk commodity chemicals such as urea and oxalic acid, which are suitable for large-scale processes. DESs form extended hydrogen-bond systems in the liquid state and are therefore highly structured "supramolecular" solvents. This special quality can be used to form well-defined, ordered nanoscale structures. Owing to the high thermal stability and low vapor pressure of DESs, reactions can be conducted at temperatures well beyond 100 °C in nonpressurized vessels. Low interface energies for particles can be translated into good stabilization. DESs are promising solvents to be used in shape-controlled synthesis of nanoparticles. However, there are as yet very few reports of the use of DESs in the synthesis of nanomaterials.[9]

Herein we report a novel route of shape-controlled synthesis of gold NPs without the use of any surfactants or seeds but with a DES as solvent. Star-shaped Au NPs that are bounded with (331) and vicinal high-index facets were successfully synthesized for the first time. The monodisperse star-shaped gold NPs were obtained directly by the reduction of $HAuCl_4$ by L-ascorbic acid at room temperature in the DES. Au NPs of various shape and surface structure including snowflake-like NPs and nanothorns can be obtained simply by adjusting the content of water in the DES. Furthermore, the electrocatalytic properties of the synthesized Au NPs were tested by using the electroreduction of H_2O_2 as a probe reaction, and it has demonstrated that the star-shaped Au NPs exhibited a much higher catalytic activity than other shaped NPs and polycrystalline Au.

The as-prepared samples were examined using scanning electron microscopy (SEM, LEO-1530). It was found that over 40% of the synthesized Au NPs exhibited regular pentagonal symmetry and displayed a striking beauty of the star-shaped particle, as illustrated in the Figure 1. The size of these Au NPs was about 300 nm. High-magnified pictures at different viewing angles (Figure S2 in the Supporting Information) illustrate that the star-shaped Au NPs are flat and have a slightly thicker center (about 90 nm). Besides the well-defined pentagonal star shape, other star-shaped Au NPs of three, four, or multiple branches are also observed in Figure 1, which may be considered as a deformation of the pentagonal star shape during crystal growth. Energy-dispersive X-ray spectroscopy (EDS) indicates that the NPs are composed of only gold (see Figure S1a in the Supporting Information). We have also traced the synthetic process by using UV/Vis

[*] Dr. H. G. Liao, Prof. Y. X. Jiang, Z. Y. Zhou, S. P. Chen, Prof. S. G. Sun
State Key Laboratory of Physical Chemistry of Solid Surfaces, Department of Chemistry, College of Chemistry and Chemical Engineering, Xiamen University
Xiamen 361005 (China)
Fax: (+86) 592-2180181
E-mail: yxjiang@xmu.edu.cn
sgsun@xum.edu.cn

[**] This work was supported by the National Natural Science Foundation of China (Grant Nos. 20433040, 20573085, and 20673091) and the "973" Program (No. 2009CB220102).

Supporting information for this article is available on the WWW under http://dx.doi.org/10.1002/anie.200803202.

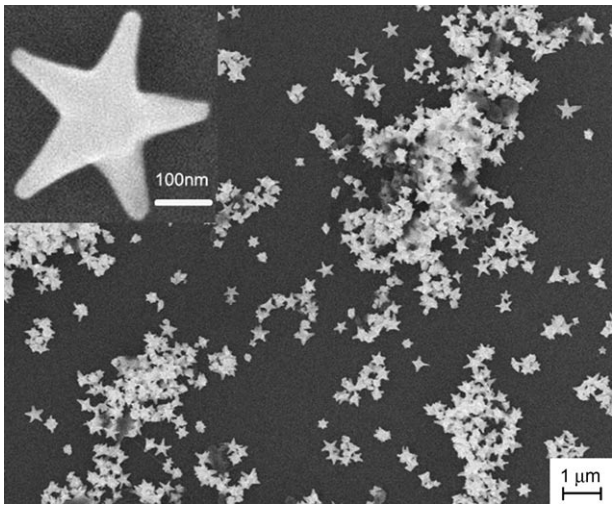

Figure 1. SEM images of the star-shaped Au NPs.

spectroscopy (see the Supporting Information for more details); the progressive shift of the absorption peak from 590 to 640 nm illustrates the formation and growth of Au NPs.

Pentagonal metal NPs with fcc structures mostly show fivefold twining structures[10] composed of five equal subunits bound together by twinned {111} planes with a deviation of the angle of a perfect twin in {111} faces (70.53°) from 360°/5 (72°). The presence of dislocations of 7.40° has been predicted as a means to adjust the lattice mismatch.

High-resolution TEM (HRTEM, TECNAI F30) images were taken at various sections in a single particle (Figure 2). These images were obtained from the [110] zone axis. Each of

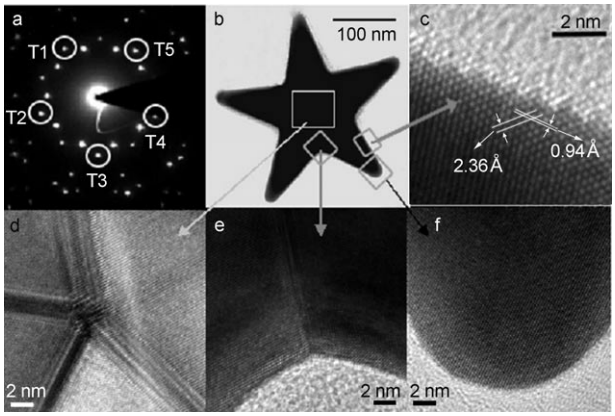

Figure 2. HRTEM images of Au NPs recorded along [110] (b–f) and the SAED pattern (a).

the twins displays single-crystal structure with well-defined intersections that can be easily assigned to twin boundaries. The fivefold twin boundaries can be seen clearly, and there seems to be inhomogeneous broadening by dislocations and stacking faults. The selected-area electron diffraction (SAED) pattern (Figure 2a) with the electron beam directed along the fivefold axis can be well interpreted by five twinned subunits with their common [110] axis. The above results proved firmly the fivefold symmetric structure of the star-shaped Au NPs.

On the basis of the results and calculations, we put forward a 3D model of these NPs (see the Supporting Information). In a perfect particle, five single crystals (T1–T5 indicated in Figure 2a) are twinned along {111} planes, and each branch of the particle is a tetragonal micro-pyramid that protrudes along the [001] direction. The four bare facets of each single crystal are high-index (331) facets. Figure 2c displays the projection of (331) facets along the [110] direction; a *d* spacing between adjacent lattice planes of 0.94 Å corresponds to the {331} planes, and 2.36 Å corresponds to the {111} planes. From Figure 2c, many atomic steps can also be observed, which confirms that the main surface facets of the five branches of the star-shaped Au NPs are those of (331) and vicinal high-index facets.

Water in the DES played a key role in the shape-controlled synthesis of Au NPs. Without water in the DES, we obtained snowflake-like gold NPs about 300 nm in size (Figure 3a). The ends of the NP branches form tetragonal micropyramids shaped like a rooftop (half an octahedron), so

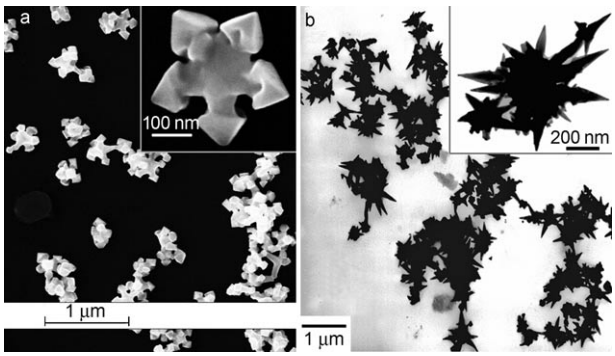

Figure 3. a) SEM images of the snowflake-like Au NPs; b) TEM images of Au nanothorns.

the main surface facets of the branch should be (111) facets.[11] When the content of water increased to 5000 ppm, star-shaped Au NPs were obtained. A large content of water (exceeding 10000 ppm) in the DES leads to the formation of nanothorns (Figure 3b). The high-magnification SEM images (Figure S5 in the Supporting Information) indicate presumably that the nanothorns have several kinds of surface facets—both high-index and low-index facets. The main effect of the DES in the synthesis may be as a liquid template as suggested in literature,[12] and the L-ascorbic acid promotes anisotropic growth.[7] The DES also acts as a stabilizer; the prepared NPs can steadily exist in DES for a period of weeks.

Sun and co-workers have shown that a Pt(331) electrode exhibited a high electrocatalytic activity towards ethylene glycol oxidation, which was attributed both to the configuration of the atomic arrangement and to the stability of this surface.[13] The star-shaped Au NPs bounded with (331) surfaces and vicinal high-index facets may also have high catalytic activity thanks to the high density of step atoms. The structure–functionality relationship was studied further by employing electrocatalytic reduction of H_2O_2 as probe

reaction; the reduction current has been normalized to electroactive Au surface area so that the current density (j) can be directly used to compare the catalytic activity of different samples. Current–potential curves of H_2O_2 reduction on different Au electrodes are compared in Figure 4. As expected, the star-shaped NPs exhibit higher catalytic activity

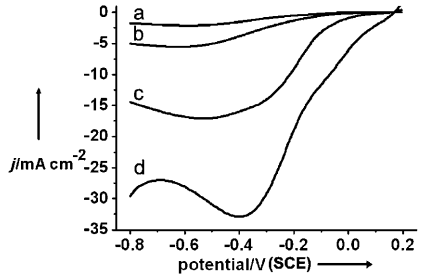

Figure 4. Current–potential curves of electrocatalytic reduction of 20 mM H_2O_2 in 0.1 M phosphate-buffered solution; scan rate 50 mV s^{-1}; a) polycrystalline Au electrode, b) snowflake-like Au NPs, c) nanothorns, d) star-shaped Au NPs.

than others. The onset potential of H_2O_2 reduction on an electrode of star-shaped Au NPs was positively shifted by about 150 mV relative to that on a polycrystalline Au electrode. The onset potential was also positively shifted by about 50 mV on the electrode of Au nanothorns, whereas on an electrode of the snowflake-like NPs it was negatively shifted by about 30 mV.

Besides the significantly positive shift of the onset potential for H_2O_2 reduction on the electrode of star-shaped Au NPs, which reveals a low activation energy, the higher catalytic activity of the star-shaped Au NPs consists also of the higher reduction current density per unit Au surface area among the investigated Au electrodes. Figure 5 shows transient current density curves of H_2O_2 reduction on different electrodes. The catalytic activity of Au NPs of different shapes is always superior to that of polycrystalline Au and is more pronounced for the star-shaped Au NPs. The reduction current density on star-shaped NPs has been enhanced to 14 times that on bulk Au. For the nanothorns and snowflake-like NPs, the enhancement in catalytic activity is 7 and 2.5 times, respectively. The largely enhanced catalytic activity of the star-shaped Au NPs comes from their high-index facets. In comparison with bulk Au, the nanothorns bounded with both

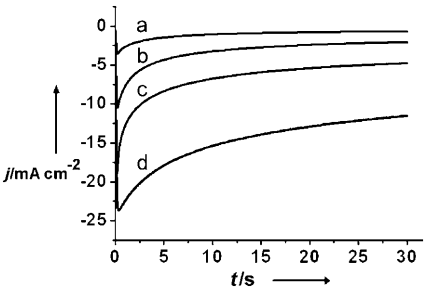

Figure 5. Transient current-density curves of 20 mM H_2O_2 reduction at −0.5 V; a) polycrystalline Au electrode, b) snowflake-like Au NPs, c) nanothorns, d) star-shaped Au NPs.

high-index and low-index facets, and the snowflake-like gold NPs are enclosed mainly with low-index (111) facets.

In conclusion, shape-controlled synthesis of Au nanoparticles was developed successfully in deep eutectic solvents. Star-shaped Au NPs were synthesized for the first time in a DES without seeds or stabilizer at room temperature. It has been demonstrated that the shape as well as the surface structure of the Au NPs may be tuned by simply varying the content of a small amount of water in the DES. The star-shaped Au NPs exhibit high catalytic activity towards H_2O_2 electrocatalytic reduction, attributed to their high-index facets, which provide a high density of stepped atoms. The variety in shape offers the opportunity to change the surface structure of nanoparticles and examine the structure–functionality relationships in electrocatalysis. Work on minimizing the size of the Au NPs has also been conducted, and our preliminary results demonstrate that smaller star-shaped gold NPs could be synthesized by adding Au seeds. The present method may be applied to carry out shape-controlled synthesis of other metal NPs.

Experimental Section

In a typical synthesis, $HAuCl_4{\cdot}4H_2O$ (0.015 g, Sinopharm chemical reagent) and L-ascorbic acid (0.05 g, Sinopharm chemical reagent) were added separately into DES (25 mL each) and stirred at 30 °C in a sealed rocked flask until they completely dissolved. The L-ascorbic acid solution was then added to the $HAuCl_4{\cdot}4H_2O$ solution with continued stirring by a magnetic agitator at 30 °C. When the content of water was about 5000 ppm, the reaction took a few hours to finish. At the end of the reaction, the color of the solution changed from yellow to dark purple. More water in the system will shorten the reaction time. The content of water in the system was measured by Karl–Fischer titration (Mettler Toledo titrators DL-32) and then adjusted by adding Milli-Q water.

In another anhydrous synthesis process, the reactant solution was prepared in a glove box, and after the flask was sealed, it was taken out and stirred with a magnetic agitator. The reaction took a week to complete.

Electrochemical experiments were carried out in a standard three-electrode cell at room temperature (about 25 °C). The DES used herein was prepared according to reference [14]. More experimental details are given in the Supporting Information.

Received: July 2, 2008
Published online: October 16, 2008

Keywords: deep eutectic solvents · electrocatalysis · reduction · shape-controlled synthesis · structure-activity relationships

[1] M. Haruta, N. kobayashi, H. Sano, N. Yamada, *Chem. Lett.* **1987**, 405 – 408.

[2] a) H. Sakurai, T. Akita, S. Tsubota, M. Kiuchi, M. Haruta, *Appl. Catal. A* **2005**, *291*, 179 – 187; b) M. S. Chen, D. W. Goodman, *Science* **2004**, *306*, 252 – 255; c) T. F. Jaramillo, S. H. Baeck, B. R. Cuenya, E. W. McFarland, *J. Am. Chem. Soc.* **2003**, *125*, 7148 – 7149; d) J. T. Zhang, P. P. Liu, H. Y. Ma, Y. Ding, *J. Phys. Chem. C* **2007**, *111*, 10382 – 10388.

[3] a) G. A. Somorjai, D. W. Blakely, *Nature* **1975**, *258*, 580; b) L. M. Molina, B. Hammer, *Appl. Catal. A* **2005**, *291*, 21 – 31; c) T. V. W. Janssens, B. S. Clausen, B. Hvolbaek, H. Falsig, C. H. Christensen, T. Bligaard, J. K. Norskov, *Top. Catal.* **2007**, *44*, 15 – 26.

[4] N. Tian, Z. Y. Zhou, S. G. Sun, Y. Ding, Z. L. Wang, *Science* **2007**, *316*, 732 – 735.
[5] a) T. K. Sau, C. J. Murphy, *J. Am. Chem. Soc.* **2004**, *126*, 8648 – 8649; b) S. Shukla, A. Priscilla, M. Banerjee, R. R. Bhonde, J. Ghatak, P. V. Satyam, M. Sastry, *Chem. Mater.* **2005**, *17*, 5000 – 5005; c) H. Y. Wu, H. C. Chu, T. J. Kuo, C. L. Kuo, M. H. Huang, *Chem. Mater.* **2005**, *17*, 6447 – 6451.
[6] O. Krichevski, G. Markovich, *Langmuir* **2007**, *23*, 1496 – 1499.
[7] J. L. Burt, J. L. Elechiguerra, J. Reyes-Gasga, J. M. Montejano-Carrizales, M. Jose-Yacaman, *J. Cryst. Growth* **2005**, *285*, 681 – 691.
[8] A. P. Abbott, D. Boothby, G. Capper, D. L. Davies, R. K. Rasheed, *J. Am. Chem. Soc.* **2004**, *126*, 9142 – 9147.
[9] a) J. H. Liao, P. C. Wu, Y. H. Bai, *Inorg. Chem. Commun.* **2005**, *8*, 390 – 392; b) E. R. Cooper, C. D. Andrews, P. S. Wheatley, P. B. Webb, P. Wormald, R. E. Morris, *Nature* **2004**, *430*, 1012 – 1016.
[10] a) A. Sanchez-Iglesias, I. Pastoriza-Santos, J. Perez-Juste, B. Rodriguez-Fernandez, F. J. Garcia de Abajo, L. M. Liz-Marzan, *Adv. Mater.* **2006**, *18*, 2529 – 2534; b) H. Y. Chen, Y. Gao, H. R. Zhang, L. B. Liu, H. C. Yu, H. F. Tian, S. S. Xie, J. Q. Li, *J. Phys. Chem. B* **2004**, *108*, 12038 – 12043.
[11] Z. L. Wang, *J. Phys. Chem. B* **2000**, *104*, 1153 – 1175.
[12] E. R. Parnham, E. A. Drylie, P. S. Wheatley, A. M. Z. Slawin, R. E. Morris, *Angew. Chem.* **2006**, *118*, 5084 – 5088; *Angew. Chem. Int. Ed.* **2006**, *45*, 4962 – 4966.
[13] S. G. Sun, A. C. Chen, T. S. Huang, J. B. Li, Z. W. Tian, *J. Electroanal. Chem.* **1992**, *340*, 213 – 226.
[14] A. P. Abbott, G. Capper, D. L. Davies, R. K. Rasheed, P. Shikotra, *Inorg. Chem.* **2005**, *44*, 6497 – 6499.

